Finite resource performance of small satellite-based quantum key distribution missions

Tanvirul Islam,[1,*] Jasminder S. Sidhu,[2,†] Brendon L. Higgins,[3,‡] Thomas Brougham,[2]
Tom Vergoossen,[4] Daniel K. L. Oi,[2] Thomas Jennewein,[3] and Alexander Ling[1,5]

[1] *Centre for Quantum Technologies, National University of Singapore, 3 Science Drive 2, 117543 Singapore*
[2] *SUPA Department of Physics, University of Strathclyde, Glasgow, G4 0NG, UK*
[3] *Institute for Quantum Computing and Department of Physics and Astronomy, University of Waterloo, Waterloo, ON N2L 3G1, Canada*
[4] *SpeQtral Pte. Ltd., 73 Science Park Drive Science Park 1, 118254 Singapore*
[5] *Department of Physics, National University of Singapore, Blk S12, 2 Science Drive 3, 117551 Singapore*

In satellite-based quantum key distribution (QKD), the number of secret bits that can be generated in a single satellite pass over the ground station is severely restricted by the pass duration and the free-space optical channel loss. High channel loss may decrease the signal-to-noise ratio due to background noise, reduce the number of generated raw key bits, and increase the quantum bit error rate (QBER), all of which have detrimental effects on the output secret key length. Under finite-size security analysis, higher QBER increases the minimum raw key length necessary for non-zero secret key length extraction due to less efficient reconciliation and post-processing overheads. We show that recent developments in finite key analysis allow three different small-satellite-based QKD projects CQT-Sat, UK-QUARC-ROKS, and QEYSSat to produce secret keys even under very high loss conditions, improving on estimates based on previous finite key bounds. This suggests that satellites in low Earth orbit can satisfy finite-size security requirements, but remains challenging for satellites further from Earth.

I. INTRODUCTION

The emergence of terrestrial quantum networks in large metropolitan areas demonstrates an increasing maturity of quantum technologies. A networked infrastructure enables increased capabilities for distributed applications in delegated quantum computing [1, 2], quantum communications [3, 4], and quantum sensing [5]. However, extending these applications over global scales is currently not possible owing to exponential losses in optical fibres. Space-based segments provide a practical route to overcome this and realise global quantum networking [6, 7]. Satellite-based Quantum Key Distribution (SatQKD) has become a precursor to long-range applications of general quantum communication [8, 9]. Although a general-purpose quantum network [10] will require substantial advancements in quantum memories and routing techniques, a satellite-based QKD system adds to the progress of global-scale quantum networks by driving the maturation of space-based long-distance quantum links.

There has been growing interest in satellite-based quantum key distribution. The recent milestone achievements by the Micius satellite [11] which demonstrated space-to-ground QKD and entanglement distribution have energized this interest. Micius, being a large satellite, leaves open the possibility of using smaller satellites to perform satellite-based QKD—there have been feasibility studies for small-satellite-based QKD and CubeSat-based pathfinder missions [12] for QKD applications.

This surge in effort emphasizes the importance of understanding specific limitations to the performance of different SatQKD systems. For low-Earth orbit (LEO) satellites, a particular challenge is the limited time window to establish and maintain a quantum channel with an optical ground station (OGS). This limitation disproportionately constrains the volume of secure keys that can be generated due to a pronounced impact of statistical fluctuations in estimated parameters.

In this work, we analyze three different mission configurations: the Singapore Centre for Quantum Technologies' CQT-Sat, the UK quantum research CubeSat/Responsive Operations for key services (QUARC/ROKS) satellite, and the Canadian quantum encryption and science satellite (QEYSSat). The quantum channel configuration for each mission is illustrated in Figure 1. Depending on the ground station location and the specific LEO orbit, a satellite may have a limited number of passes over the OGS for which QKD key generation is possible—for example, current technology requires that passes are conducted during nighttime. Therefore, it is important to understand the conditions that allow a SatQKD system to produce secret keys successfully from a single pass over the OGS. More specifically, for any given satellite pass, how many secret key bits can be generated? We answer this for the three mission configurations by revisiting the supporting theory and modelling of key generation [13–17]. It is shown that all three missions demonstrate enhanced key generation with the latest advancements in finite key analysis. We conclude by looking at the prospects for satellites at higher altitude where the longer access time for a ground receiver does not overcome the increased diffraction loss.

* cqtmti@nus.edu.sg; These authors contributed equally
† jsmdrsidhu@gmail.com; These authors contributed equally
‡ brendon.higgins@uwaterloo.ca

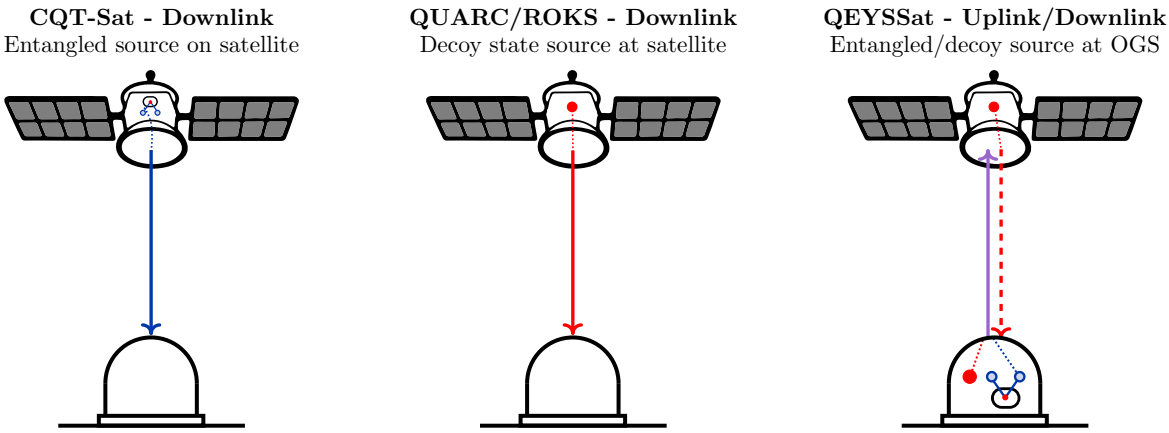

FIG. 1. Quantum channel configuration for three different SatQKD missions. Each mission implements a different combination of QKD protocols and quantum channel configurations between an OGS and an orbiting satellite. The Singaporean CQT-Sat mission (left) implements the entanglement-based BBM92 protocol (blue arrow) in a downlink configuration. For this mission, one of the photon pairs is measured on board and the other is transmitted to the OGS. The UK QUARC/ROKS mission (middle) implements the WCP decoy-state BB84 protocol (red arrow) in a downlink configuration. The Canadian QEYSSat mission (right), implements both the decoy BB84 and BBM92 protocols (purple arrow) in an uplink configuration and intends to also incorporate a decoy BB84 downlink.

II. SATELLITE-TO-GROUND ENTANGLEMENT-BASED QKD USING BBM92

CQT-Sat is a 12U nano-satellite capable of performing space-to-ground entanglement-based QKD. Its precursor SpooQy-1 demonstrated [12] successful launch and operation of a miniaturized polarization-entangled photon pair source in LEO. The subsequent payload will build upon this to perform space-to-ground entanglement distribution and demonstrate entanglement-based BBM92 QKD.

During a satellite's overpass over the ground station, the link loss for the downlink quantum channel will depend on the relative distance between the satellite and the OGS. Using a variable attenuator, a tabletop setup can emulate a time-varying satellite-to-ground link loss (a similar experiment was conducted previously in the context of QEYSSat [18]). This enables us an estimation of the achievable raw key length and overall QBER for various satellite passes. Using these parameters we perform finite key analysis and show that CQT-Sat can successfully generate shared secret keys between the satellite and OGS when the maximum elevation is as low as 33°.

A. System configuration

The satellite quantum source generates polarization-entangled photon pairs by superposing orthogonally polarized photons created from spontaneous parametric down-conversion using two pump decay paths [19]. Detailed design of a functional model of the source and associated design trade-offs can be found in [20]. The source generates pairs of polarization-entangled photons where each pair consists of a 785 nm wavelength signal photon and an 837 nm wavelength idler photon. For the purpose of QKD, each of the idler photons is measured aboard the satellite in either the computational or the diagonal basis with probability 1/2. The signal photon is sent to the satellite's optical terminal using an optical interface. A subsystem inside the optical source also generates a synchronization beacon. Both the beacon and the signal photons are transmitted to the OGS through the satellite's optical terminal.

Optical terminals both on the satellite and in the ground station facilitate establishing a space-to-ground free-space optical link. They consist of optical telescopes and fine pointing mechanisms for transmitting and collecting the signal photons, and synchronization and tracking beacons. Table I presents the parameters of the quantum source and the optical link.

B. Emulating space-to-ground QKD using a tabletop setup

To emulate a space-to-ground QKD link we built the entanglement source and the detection apparatus representative of both the satellite and ground systems. The system parameters for this setup is listed in Table II.

We consider a Sun synchronous low Earth orbit with 500 km altitude above sea level. This orbit choice gives us daily passes over our ground station at a pre-specified time of the day [21]. We compute a time series of the satellite's angular elevation with respect to the OGS and the loss at that elevation for a pass. For example, in Figure 2 we show a pass with 88° maximal elevation and associated loss that the optical link experiences.

Using a variable attenuator we introduce different losses, and record detection timestamps for both signal

Parameter	Value	Description
Transmitter aperture	0.09 m	Realistic aperture size for nanosatellite
Receiver aperture	0.6 m	Optimum aperture
Beam quality	1.6 M2	Fundamental limit is 1.4 due to diffraction
Atomspheric attenuation	3 dB	3 dB at zenith, scaled with path length for lower elevation
Pointing jitter	5 microrad	1.2 microrad demonstrated on Micius satellite
Efficiency	50 %	Estimated based on reflectivity and number of optical surfaces
Background counts	1300 cps	Measured with respective setup in Singapore

TABLE I. Space-to-ground optical link parameters for CQT-Sat.

System Parameter	Value
Entangled pair production rate	20 Mcps
Source intrinsic QBER	0.91 %
Signal wavelength	785 nm
Idler wavelength	837 nm
Bandwidth	5 nm
Detection efficiency	25 %
Dark count rate per detector	500 cps
Detector dead time	50 ns
Detection jitter	320 ps
Detector after-pulsing probability	5 %

TABLE II. Source and detector parameters for CQT-Sat.

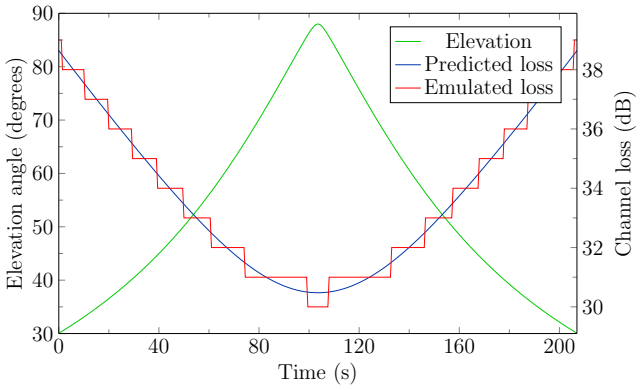

FIG. 2. Example simulated satellite pass reaching 88° elevation angle (green line). Experimental data is assembled such that its loss profile (orange line) closely matches the theoretically predicted optical loss (blue line).

and idler photons. Due to physical limitations, we only use a finite number of attenuator settings, and stitch the experimental data together to emulate the predicted loss of the optical downlink. The blue and orange lines in Figure 2 illustrate the predicted and experimentally-emulated loss respectively at various segments of the satellite pass.

This technique allows the investigation of satellite passes with different maximum elevations and to generate the associated detection timestamps both on-board the satellite and in the OGS. These timestamp sets are processed through the rest of the QKD protocol stack including finite key analysis to compute the secure key length achievable from each pass.

C. Key length of CQT-Sat for various LEO satellite passes

Depending on geographical location and satellite orbit, a ground receiver might observe 2 to 6 satellite passes each day. An ideal satellite pass would transit directly over the ground station with maximal elevation of 90° (zenith). At zenith, the satellite is closest to the OGS, and in clear weather this pass would exhibit the lowest transmission loss and longest link time. However, such a pass is less likely than more "glancing" passes. For a given detector dark count rate, higher losses would result in a poorer signal-to-noise ratio and increase the QBER. Moreover, the pass duration and the number of photons successfully received from the satellite also decrease. Figure 3 shows how the secret key length changes with different satellite passes. Here we use the finite key analysis from [17] taking security parameter 10^{-10} where error correction efficiency is 1.18.

The analysis shows that below an elevation of 30° no secret key is generated. This is acceptable for CQT-Sat which was designed to avoid operation at low elevation. The ground receiver in this case is sited at sea level in a tropical, urban environment and the optical channel below 30° is extremely lossy due to the thicker atmospheric column. Additional light pollution at low elevation is much more severe, contributing to increased noise.

III. SATELLITE-TO-GROUND QKD USING DECOY-STATE BB84

The UK Quantum Research CubeSat (QUARC) project provides a design and architectural foundation for the Responsive Operations for Key Services (ROKS) mission in the National Space Innovation Programme (NSIP) [22, 23]. ROKS uses a continuation of the same 6U CubeSat platform as QUARC and will first implement decoy-state BB84 protocol in a downlink configuration for QKD service provision using a weak coherent pulse (WCP) source (Figure 1).

The satellite quantum modelling and analysis

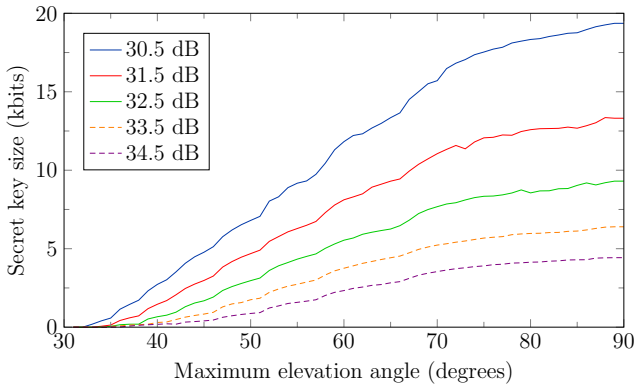

FIG. 3. Secret key length achievable for passes of given maximal elevation. The blue curve gives results for the default simulation where the minimum loss at zenith is 30.5 dB. Other curves show behaviour for optical links with additional 1 to 4 dB losses. Solid lines are based on experimental data constructed to emulate pass loss profiles. Dashed curves were simulated numerically.

Parameter	Value	Description
Intrinsic error	0.5%	Source errors
After-pulsing	0.1%	Probability of p_{ap}
Extraneous count rate	5×10^{-7}	Probability of counts from background light
Source rate	100 MHz	Signal frequency
Error correction	10^{-15}	Error-correction efficiency
Security	10^{-9}	Security parameter
Altitude	500 km	Satellite orbit altitude
System loss	34 dB	Loss at zenith

TABLE III. Reference system parameters. We take published information of the Micius satellite and OGS system as representing an empirically derived set point for our finite key analysis. The total loss at zenith can be linearly scaled to model other systems with smaller OGSs or differing source rates.

(SatQuMA) open-source software has been developed to estimate expected key generation performances for such satellite QKD missions [24]. SatQuMA models the efficient BB84 weak coherent pulse (WCP) two-decoy (three intensity) protocol and can optimise over the entire protocol parameter space and transmission segment time. It also incorporates recent results in finite-block composable secure key length estimation [17, 25, 26]. SatQuMA can be applied to model the expected key generation performance for ROKS for a general satellite pass geometry in a Sun-synchronous orbit (SSO) at altitude h.

A. System configuration

We use published empirical Micius mission measurements of the total optical loss of the SatQKD channel [27] to construct a representative total system link efficiency as a function of elevation angle during a satellite pass. To account for local horizon constraints around the OGS, we restrict quantum transmissions to elevations above 10°. The simplest type of orbit is the zenith pass, where the satellite flies directly over the OGS, reaching a maximum elevation of 90°.

The link efficiency (loss) is highly dependent on the system parameters, OGS conditions, and orbits. The nominal system parameters are summarized Table III, where the minimum total system loss at zenith is computed to be 34 dB. One can scale the minimum system loss at zenith to allow the comparison of differently performing SatQKD systems. Changes to the minimum system loss at zenith would then account for differences in the transmit and receive aperture sizes, pointing accuracy, atmospheric absorption, turbulence, receiver internal losses, and detector efficiencies. For the current simulations, we consider a nominal baseline value of 34 dB. SatQKD missions with differing performance can be modelled by linearly scaling the link efficiency vs elevation curve to account for different constant efficiency factors, such as a change in OGS receiver area.

To evaluate the sensitivity of the achievable secret key length to different errors, we categorise different contributions associated with sources and detectors in two key parameters. First, errors from dark counts and background light are combined together into a single extraneous count probability p_{ec}, here assumed to be constant and independent of elevation. In practice, it will depend strongly on the environment of the OGS and light from celestial bodies. Second, all other error terms, such as misalignment, source quality, imperfect detection, are combined into an intrinsic quantum bit error rate QBER_{I} independent of channel loss/elevation. This allows an efficient method to determine the sensitivity of the secret key length to different categories of errors, which helps identify targeted improvements for future SatQKD missions. All of the nominal system parameters are summarised in Table III.

B. Optimised finite key length

We model the efficient BB84 protocol, adopting the convention of key generation using signals encoded in the X basis and parameter estimation using signals in the Z basis, chosen with biased probabilities. For a two-decoy-state WCP BB84 protocol, one of three intensities μ_j for $j \in \{1, 2, 3\}$ are transmitted with probabilities p_j. An expression for the final finite key length, ℓ, for this protocol is given in Ref. [13]. The key is extracted from data for the whole pass as a single block without partitioning, the security proof of Ref. [13] makes no assumptions about the underlying statistics. This avoids having to combine small data blocks with similar statistics from different

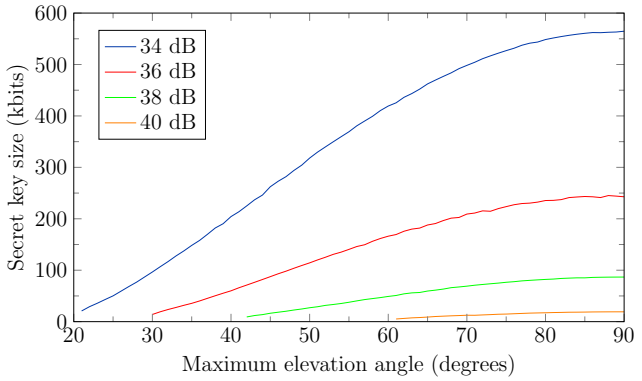

FIG. 4. Estimated secret key length generated by QUARC mission for passes with different maximum elevation angles. In the default simulation the minimum total system loss is 34 dB. Other curves show behaviour for optical links with additional 2, 4, and 6 dB losses.

passes—thus, it is both quicker and avoids the need to track and store a combinatorially large number of link segments until each has attained a sufficiently large block size for asymptotic key extraction.

The limited data sizes from restricted pass times results in key length corrections to account for finite statistics of the link. To improve the analysis, we use the tight multiplicative Chernoff bound [16] and improve the estimate of error correction leakage $\lambda_{\mathrm{EC}} \leq \log|\mathcal{M}|$, where $\mathcal{M}$ characterises the set of error syndromes for reconciliation [14] (see Ref. [25] for more details).

For a defined SatQKD system, we optimise the finite key length ℓ by optimising over the protocol parameter space that includes the source intensities (with $\mu_3 = 0$) and their probabilities, and the basis encoding probability p_{X}. We also optimise over the portion of the pass data used for key generation. To efficiently handle this optimisation, we developed a numerical toolkit to numerically analyse different SatQKD systems. The satellite quantum modelling and analysis (SatQuMA) software assists in developing an intuition about the effects of different operational scenarios on the key rate, to better inform the development of source and receiver systems for future satellite missions [24].

The SatQuMA code is used to generate simulated measurement data. The QBER and phase errors for the key bits are estimated using only the data for the complementary basis. This is a classic sampling without replacement problem, which is usually solved in QKD using an approximation for the hyper-geometric distribution [28]. Recently, however, an improved sampling bound has been proposed [17]. This can be used to estimate the QBER and phase error. The formalism from Ref. [17] is used together with data generated from SatQuMA to determine the secret key length for different satellite passes, which we characterize through the maximum elevation angle. The secret key is plotted in Figure 4 as a function of the maximum elevation angle of a pass.

IV. SATQKD USING BBM92 IN UPLINK OR DOWNLINK CONFIGURATIONS

The Quantum Encryption and Science Satellite (QEYSSat) mission [29] is a Canadian initiative to develop and launch a microsatellite-hosted quantum receiver payload into low-Earth orbit. The primary objective of the mission is to demonstrate QKD via quantum uplink from sources located at two or more ground stations. To support this, the QEYSSat payload will possess a large front-end telescope for light collection, polarization discriminating optics, and single-photon avalanche diodes [30]. Support for a WCP downlink protocol is also being developed. As of writing, QEYSSat is in the late design/early construction phase and on schedule to launch in 2023/2024.

A. System configuration

With QEYSSat's nominal configuration being an uplink, and the quantum sources located on the ground, lower secure key rates are expected when compared to a downlink with equivalent parameters, owing to the steering effect of turbulent atmosphere on the beam at the beginning of its propagation (in contrast to the end of propagation for a downlink). However, a satellite receiver affords considerably greater source flexibility. For this reason, two source types are baselined: WCP with decoy states in an unbiased BB84 protocol, and entangled photons (with one photon of each pair kept at the ground) in a BBM92 protocol. It is expected that other quantum source types—e.g., quantum dots (see, e.g., Ref. [31])—will also be employed during the experimental phase of the QEYSSat mission.

Commencement of the QEYSSat mission in 2018 was preceded by several theoretical and experimental investigations into the mission's feasibility, both as a whole [32] and with focus on critical subsystems including pointing [33, 34] and photon measurement [35, 36]. Of these, one early work [37] numerically modelled the quantum optical link to establish the loss and fidelity of polarized-photon transmission under the assumptions of the expected orbital configuration and (generally conservative) atmospheric conditions. Multiple scenarios were considered, consisting of notional WCP or entangled-photon sources in both uplink and downlink configurations. Although some details of the in-development QEYSSat apparatus and conditions have been refined since, the values remain generally very similar. In this work we present secret key generation performance of QEYSSat while executing the entanglement-based BBM92 protocol in both satellite-to-ground (downlink) and ground-to-satellite (uplink) quantum communication configuration modes.

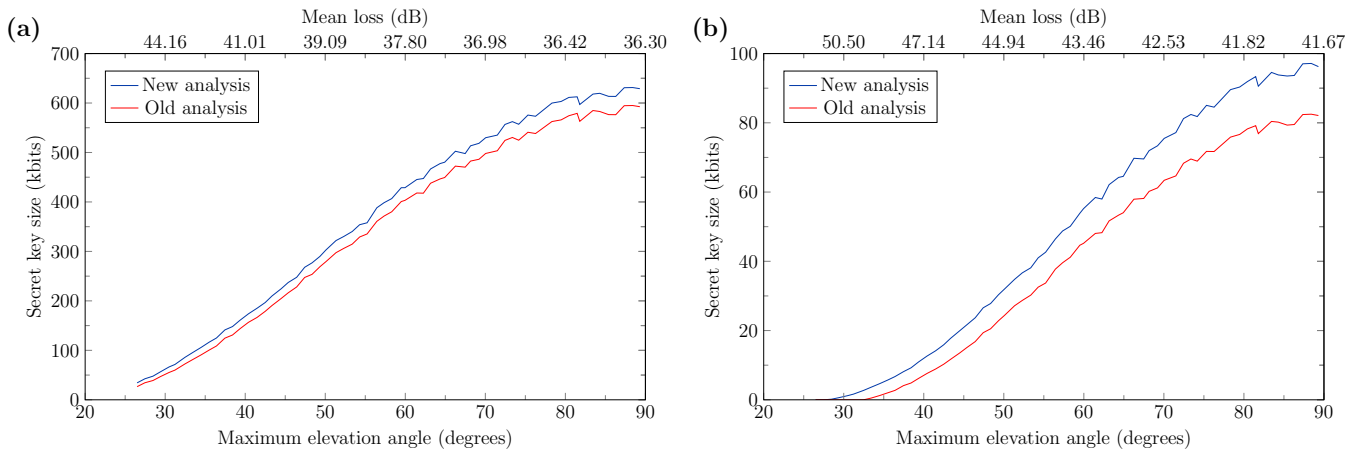

FIG. 5. Expected performance of representative conditions modelled for QEYSSat performing entanglement based QKD in (a) Entanglement based satellite-to-ground downlink and (b) Entanglement based ground-to-satellite uplink configurations. Newer finite key analysis yields improved secure key lengths.

B. Key length analysis

In the prior analysis [37], calculations were performed using secure key rate equations which were well-established at that time—for comparison, we reproduce those calculations, with minor corrections found since publication, error correction efficiency improved to 1.18 (originally 1.22), and security parameter 10^{-9}.

More significantly, here we determine the expected secure key lengths with the same quantum transmission and fidelity profiles (corresponding to the same conditions being modeled) using updated secure key length analysis [17] which has improved performance with smaller raw key block size. Performance with smaller block size is important because it has implications on QKD feasibility under high-loss conditions and during low maximum elevation passes.

Table IV summarizes the parameters that describe the quantum source and the optical link. The assumed satellite orbit (Sun-synchronous noon/midnight at 600 km altitude) was simulated for one year's duration of nighttime passes over a notional ground station located 20 km outside of Ottawa, Canada. Optical link conditions for each pass were modeled at ten-second intervals. Background light was determined from the Defence Meteorological Satellite Program's Operational Linescan System measurements and combined with an assumed half-moon at 45° (contributing via Earth reflection using its mean albedo) along with Earth's thermal (blackbody) radiation, taking into account the geometry of the optical field of view and 1-nm-bandwidth spectral filtering. Detector dark counts were also included.

The study considered various transmitter and receiver diameters, while 50 cm and 30 cm, respectively, were baselined and will be assumed here. Optical losses were calculated from the contributions of numerically modeled diffraction given a central obstruction (secondary mirror), an assumed mean pointing error of 2 microrad, atmospheric attenuation modeled by MODTRAN 5 for a "rural" profile with 5 km visibility, and Hufnagel–Valley model of atmospheric turbulence at sea-level. Photonic states were simulated in a 7-dimensional Fock-space (0 to 6 photons). Intrinsic reduction in quantum visibility was included via an operation equivalent to a small rotation.

Parameter	Value
Orbital altitude	600 km
Transmitter aperture	0.5 m
Receiver aperture	0.3 m
Pointing error	2 microrad
Optics losses	3 dB
Quantum transmission wavelength	785 nm
Detector loss	2.3 dB
Spectral filtering bandwidth	1 nm
Dark count rate per detector	20 cps
EPS pair production rate	100 Mcps
Source intrinsic QBER	1%
Coincidence window	0.5 ns

TABLE IV. Ground-to-space optical link parameters for the model representing QEYSSat.

Detector count rate statistics were calculated using assumed EPS pair production rate of 100 Mpairs/s and a 0.5 ns coincidence window. Intervals where the simulated measurement visibility was below 85% were filtered out (see Ref. [38]). For the present analysis, we aggregated the remaining statistics at each pass, and sorted these by the maximum elevation achieved by the satellite with respect to the ground station for that pass.

In Figure 5(a) and (b) we show the secret key generated for passes with different maximum elevation in the downlink and uplink configurations respectively for

entanglement-based BBM92. For the new results we use the finite key analysis form from Ref. [17], with stricter security parameter 10^{-10} and error correction efficiency 1.18 to compute the secure key lengths. Notably in the uplink case, the new analysis techniques achieve almost 1/4 better key lengths for the same losses near zenith, while also accessing positive key lengths for passes with lower maximum elevations than the old analysis could tolerate (even with its more lenient 10^{-9} security parameter). We may also compare these results with the CQT-Sat downlink scenario where finite key analysis is performed with the same parameters. Notably, the secret key size is considerably greater—we expect this is largely a consequence of the faster source rate and assumed enhancements to intrinsic QBER and pointing accuracy, coupled with the highly nonlinear effect of finite-size statistical analysis.

V. COMPARISONS

As the three SatQKD missions discussed here have different design specifications for the ground stations, satellites, and the protocols implemented, a direct quantitative performance comparison of the missions is difficult. Despite this, we provide a qualitative discussion on the respective strengths and weaknesses of each missions. First, the uplink configuration employed by QEYSSat has the advantage that it relieves the source design from the strict SWaP constraint imposed by a satellite. Moreover, it potentially allows QEYSSat to swap the entanglement source to a prepare and measure source at any point of the mission to perform a different SatQKD protocol. However, it has a disadvantage that the optical link suffers larger environmental turbulence during the initial part of the optical path, generating higher beam wandering compared to a downlink configuration.

The QUARC/ROKS mission uses a prepare and measure decoy state BB84 protocol where the source emits a periodic signal. This allows higher repetition rates to achieve larger raw key rates to counter for the loss experienced in the satellite-to-ground optical link. In addition to a higher performance requirement for the detection and time-stamping circuits, the repetition rate is also constrained by the speed of quantum random number generation for choice of quantum signal transmission. A similar attempt to counter the link loss by increasing brightness of an entanglement source quickly hits a bottleneck because the SPDC based source does not produce periodic signals, therefore due to finite resolution of time-stamping devices and the limits imposed by detector jitters the source ends up producing too many multi-photon events per time-slot increasing the QBER to an unacceptable value. However, entanglement based QKD implementations act as precursors to entanglement-sharing links, which are essential for future development towards a general-purpose quantum internet.

VI. CHALLENGES AND OUTLOOK

The preceding sections show that an individual small satellite can satisfy finite-key requirements for SatQKD. While an individual satellite in an appropriately chosen orbit can cover the Earth's surface each day, increased performance in the network will probably require constellations of these satellites [39]. Aside from putting more satellites into space, it is important to consider how the performance of each individual satellite could be enhanced. From the preceding discussion, it is clear that LEO satellites are working at the edge of performance in terms of SatQKD that satisfy finite-key security. It would be desirable to have continued development to the efficiency of finite-key security in the future. This would enable existing technology to deliver enhanced key rates. Aside from improvements in finite-key analysis, in which direction should development efforts proceed in order to improve SatQKD performance?

A conventional research programme would revolve around improved transmitters and detectors. We propose that building a system that can operate effectively in daylight would be a major step. Practically, every SatQKD mission for the foreseeable future will operate during nighttime to avoid excess background light from the Sun. In order to operate during daylight, the spectral window of the transmitted light has to be sufficiently narrow for effective filtering, while the transmission system on the satellite has to be built to avoid reflecting sunlight directly to the ground receiver. We note that adaptive optics (AO) for the optical ground receiver [40–42], to effectively couple light into a single mode fiber for direct transmission of the QKD signal to end-users located away from the ground receiver, will also become increasingly important. This has the added advantage that an adaptive optics system will act as a spatial filter, reducing the amount of stray light entering the quantum channel. To be useful, the AO system will need to be able to operate with high coupling efficiency, so that the overall system throughput is not compromised. Research into transmission and detection systems that can penetrate cloud and fog would also be highly desirable.

Aside from the transmitter and detector aspects we note that a major loss contribution is the diffraction of the beam from the satellite. This loss could be mitigated using several different approaches. First is to operate the spacecraft at Very Low Earth Orbit (VLEO). This orbit has a nominal altitude below the International Space Station (approximately 400 km), and is often not considered due to satellites experiencing significant drag and re-entry into the Earth's atmosphere within a year. However, with space propulsion systems being developed for station keeping [43, 44], this approach may become feasible and would afford significantly lower losses owing to shorter optical links. In designing a VLEO system, factors such as micro-buffeting from the residual atmosphere, degradation from atomic oxygen, and the shorter overhead time of the satellite remain open challenges.

Second is the use of larger transmit/receive apertures. The use of larger apertures has been the primary route to minimise link loss, with a doubling in aperture sizes providing 6 dB improvements [25]. However, apertures are restricted for small satellites. Recent efforts rely on deployable and active optics [45–47].

Finally, diffraction losses can also be mitigated by developing larger and more capable satellites at very high altitudes. The advantage is that such satellites can be equipped with large transmit apertures, while increasing the ground coverage area as well as improving access time for a ground receiver. The drawback is a dramatic increase in diffraction loss that must be compensated by enlarging the transmit/receive aperture and improving pointing accuracy.

We can model the performance of SatQKD systems for varying orbital altitudes, by imposing similar capability on the satellites. The result for LEO, Medium Earth Orbit (MEO) [48] and Geostationary Orbit (GEO) [49] demonstrates the range of link losses that will be encountered. Using the receiver (ground-based) and sender (onboard-satellite) telescope, and beam parameters as shown in Table V we study the space-to-ground optical link loss (Figure 6) for higher altitude orbits. We see that the optical link loss increases rapidly with the increase in altitude as expected from the beam expansion. Therefore, to successfully perform SatQKD at higher orbits we would need to compensate by increasing parameters such as the sending or receiving telescope's aperture and pointing accuracy. In Figure 7 we see a trade-off heat-map where the satellite's transmitter telescopes aperture and pointing accuracy are varied to show how it affects the transmission for a satellite in low Earth orbit (LEO), medium Earth orbit (MEO) and geostationary orbit (GEO). From these trade-off calculations, we see that for orbits higher than LEO it is not sufficient to only change the satellite's parameter to achieve the transmission gain necessary for successful SatQKD. For higher altitudes, one would also need to improve other parameters, such as the ground telescope's aperture and pointing accuracy, and detector efficiencies.

Due to increased loss at higher altitude orbits, obtaining a secure key from a single pass over a ground station may not be possible in these cases. However, it is possible to accumulate the raw key bits over multiple passes,

Parameter	Value
Beam waist to aperture ratio	0.89
Beam	10.8 microrad
Satellite transmitter aperture	0.1 m
Pointing error	2.5 microrad
Ground receiver aperture	0.6 m
Wavelength	785 nm
Atmospheric attenuation at zenith	3 dB

TABLE V. Space-to-ground optical link parameters used for modeling higher altitude orbits.

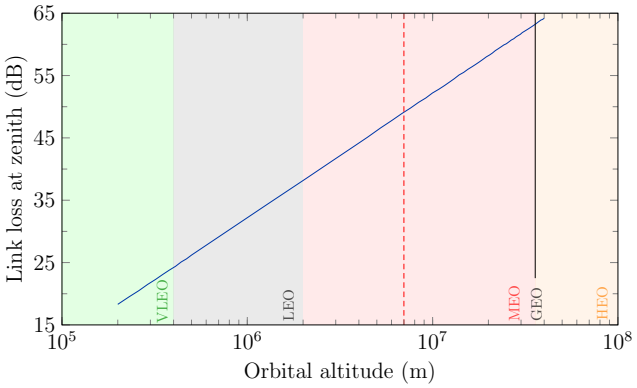

FIG. 6. Link loss as a function of orbital altitude using parameters from Table V. Green shaded region indicates altitude range for VLEO orbits, gray for LEO orbits, red for MEO orbits, orange for HEO, and the solid black line for a GEO orbit. The red dashed line corresponds to a representative MEO altitude of 7×10^3 km that we consider later. Link loss at zenith rapidly increases with increasing orbital altitudes.

increasing the block size to reduce finite block size effects sufficiently to achieve a secure key. In Figure 8 we see the block sizes and associated QBERs for the raw key bits accumulated over an year for entanglement based SatQKD operated at various orbital altitudes. The drawback of key aggregation is that large amounts of data will have to be stored for a long time onboard the satellite which might introduce vulnerabilities due to storage security. In Figure 8, we discard passes that yield QBER higher than 11%, which generates a key with minimal information known to an eavesdropper after post-processing [50]. However, given the limited number of bits acquired at each pass it might not be feasible to determine the QBER reliably by exchanging subset of these bits between the satellite and the OGS.

VII. CONCLUSION

There is growing interest in deploying satellites to enable a global QKD network. To ensure this goal remains feasible and to guide experimental and engineering efforts, it is crucial to understand how SatQKD can yield efficient secret key generation under finite transmission times and high loss regimes. Previous works have shown that secret key generation with SatQKD is possible using finite-key analyses. Recent advancements in the treatment of finite key effects have improved the efficiency of key extraction, which greatly diminishes the requirements on the minimum raw key length required for key extraction.

We use these latest finite key bounds in the most current performance analyses of three different mission concepts; the 12U CQT-Sat mission implementing an entanglement-based BBM92 downlink, the 6U QUARC project implementing a WCP decoy-state BB84 in downlink configuration, and the QEYSSat mission implement-

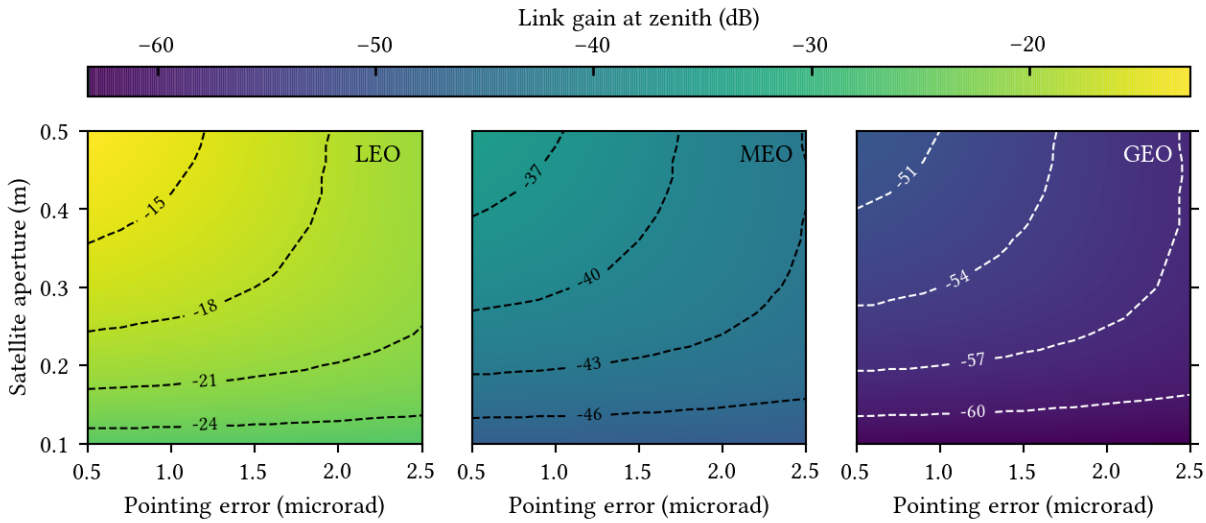

FIG. 7. Trade-off between telescope aperture onboard the satellite and pointing error with respect to the the link gain at zenith. (a) The trade-off for a representative low Earth orbit (LEO) at altitude 500 km. (b) The trade-off for a representative medium Earth orbit (MEO) at altitude 7000 km. (c) The trade-off for a geostationary orbit (GEO).

ing both the decoy BB84 and BBM92 protocols in an uplink configuration, in addition to a decoy BB84 state downlink. All three SatQKD missions achieve good secure key yields on the order of kilobits from a single pass over a ground receiver, even for the missions based on resource-constrained and aperture-limited CubeSats. This provides reassurance that planned SatQKD missions are on course to achieve key milestones that can lead to an effective global QKD network.

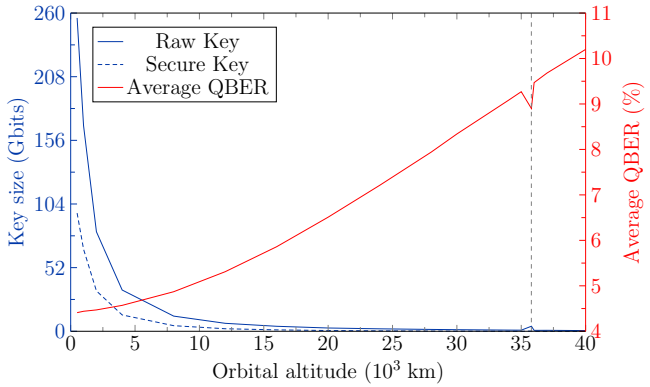

FIG. 8. Raw key length (solid blue line) accumulated over a year and average QBER (red line) as a function of orbital altitude. The dashed blue line gives the secure key extracted from the accumulated raw key block. The gray dashed vertical line indicates a GEO altitude, where the satellite remains stationary at the zenith leading to a higher raw key and lower QBER compared to other nearby orbits where the satellite has varying angular elevation with respect to the OGS during an overpass. To model this, we assume satellites telescope with aperture 0.5 m, OGS telescope with aperture 1.8 m and the entangled pair production rate 100 Mcps.

The long-term vision of a satellite-based global quantum network remains a principal motivation behind SatQKD. However, developing the infrastructure for a global QKD network sets the stage for future theoretical, experimental, and engineering milestones. Multiple OGSs should cooperate with a constellation of satellites to improve the reliability of general applications beyond QKD services. The height of technological difficulty is to realise quantum computing networks that implement full error correction [8, 10]. This will require a constellation of satellites, each synchronised and equipped with entanglement sources and quantum memories to dynamically create multi-link connections between any two points on Earth. While our calculations demonstrate that all three LEO SatQKD missions considered here have the ability to yield secure finite keys, it is clear that overcoming numerous hardware challenges and further improving security analyses simultaneously are required to establish global quantum communications.

ACKNOWLEDGMENTS

J.S.S, T.B. and D.K.L.O. acknowledge support of the UKNQTP and the Quantum Technology Hub in Quantum Communications (EPSRC Grant EP/T001011/1). B.L.H. and T.J. acknowledge support from the Canadian Space Agency, and thank J.-P. Bourgoin for discussions. T.I. and A.L. acknowledge support from the Research Centres of Excellence programme supported by the National Research Foundation (NRF) Singapore and the Ministry of Education, Singapore.

[1] A. Yimsiriwattana and S. J. L. Jr., "Distributed quantum computing: a distributed shor algorithm," in *Quantum Information and Computation II* (E. Donkor, A. R. Pirich, and H. E. Brandt, eds.), vol. 5436, pp. 360 – 372, SPIE, 2004.

[2] R. Van Meter and S. J. Devitt, "The path to scalable distributed quantum computing," *Computer*, vol. 49, no. 9, pp. 31–42, 2016.

[3] C. Liorni, H. Kampermann, and D. Bruß, "Quantum repeaters in space," *New J. Phys.*, vol. 23, p. 053021, may 2021.

[4] J. Wallnöfer, F. Hahn, M. Gündoğan, J. S. Sidhu, F. Krüger, N. Walk, J. Eisert, and J. Wolters, "Simulating quantum repeater strategies for multiple satellites," *arXiv preprint arXiv:2110.15806*, 2021.

[5] J. S. Sidhu and P. Kok, "Geometric perspective on quantum parameter estimation," *AVS Quantum Science*, vol. 2, p. 014701, February 2020.

[6] M. Gündoğan, J. S. Sidhu, V. Henderson, L. Mazzarella, J. Wolters, D. K. Oi, and M. Krutzik, "Proposal for space-borne quantum memories for global quantum networking," *npj Quantum Information*, vol. 7, p. 128, August 2021.

[7] M. Gündoğan, T. Jennewein, F. K. Asadi, E. D. Ros, E. Sağlamyürek, D. Oblak, T. Vogl, D. Rieländer, J. Sidhu, S. Grandi, L. Mazzarella, J. Wallnöfer, P. Ledingham, L. LeBlanc, M. Mazzera, M. Mohageg, J. Wolters, A. Ling, M. Atatüre, H. de Riedmatten, D. Oi, C. Simon, and M. Krutzik, "Topical white paper: A case for quantum memories in space," *arXiv*, November 2021.

[8] J. S. Sidhu, S. K. Joshi, M. Gündoğan, T. Brougham, D. Lowndes, L. Mazzarella, M. Krutzik, S. Mohapatra, D. Dequal, G. Vallone, P. Villoresi, A. Ling, T. Jennewein, M. Mohageg, J. G. Rarity, I. Fuentes, S. Pirandola, and D. K. L. Oi, "Advances in space quantum communications," *IET Quantum Communication*, vol. 2, no. 4, pp. 182–217, 2021.

[9] A. Belenchia, M. Carlesso, Ö. Bayraktar, D. Dequal, I. Derkach, G. Gasbarri, W. Herr, Y. L. Li, M. Rademacher, J. Sidhu, D. K. Oi, S. T. Seidel, R. Kaltenbaek, C. Marquardt, H. Ulbricht, V. C. Usenko, L. Wörner, A. Xuereb, M. Paternostro, and A. Bassi, "Quantum physics in space," *Physics Reports*, vol. 951, pp. 1–70, 2022.

[10] S. Wehner, D. Elkouss, and R. Hanson, "Quantum internet: A vision for the road ahead," *Science*, vol. 362, no. 6412, p. eaam9288, 2018.

[11] P. Jianwei, "Progress of the quantum experiment science satellite (QUESS) Micius project," *Chin. J. Space Science*, vol. 38, no. 5, pp. 604–609, 2018.

[12] A. Villar, A. Lohrmann, X. Bai, T. Vergoossen, R. Bedington, C. Perumangatt, H. Y. Lim, T. Islam, A. Reezwana, Z. Tang, *et al.*, "Entanglement demonstration on board a nano-satellite," *Optica*, vol. 7, no. 7, pp. 734–737, 2020.

[13] C. C. W. Lim, M. Curty, N. Walenta, F. Xu, and H. Zbinden, "Concise security bounds for practical decoy-state quantum key distribution," *Phys. Rev. A*, vol. 89, p. 022307, February 2014.

[14] M. Tomamichel, J. Martinez-Mateo, C. Pacher, and D. Elkouss, "Fundamental finite key limits for one-way information reconciliation in quantum key distribution," *Quant. Inf. Proc.*, vol. 16, p. 280, October 2017.

[15] Z. Zhang, Q. Zhao, M. Razavi, and X. Ma, "Improved key-rate bounds for practical decoy-state quantum-key-distribution systems," *Phys. Rev. A*, vol. 95, p. 012333, January 2017.

[16] H.-L. Yin, M.-G. Zhou, J. Gu, Y.-M. Xie, Y.-S. Lu, and Z.-B. Chen, "Tight security bounds for decoy-state quantum key distribution," *Sci. Rep.*, vol. 10, p. 14312, August 2020.

[17] C. C.-W. Lim, F. Xu, J.-W. Pan, and A. Ekert, "Security analysis of quantum key distribution with small block length and its application to quantum space communications," *Physical Review Letters*, vol. 126, no. 10, p. 100501, 2021.

[18] J.-P. Bourgoin, N. Gigov, B. L. Higgins, Z. Yan, E. Meyer-Scott, A. K. Khandani, N. Lütkenhaus, and T. Jennewein, "Experimental quantum key distribution with simulated ground-to-satellite photon losses and processing limitations," *Phys. Rev. A*, vol. 92, p. 052339, 2015.

[19] A. Anwar, C. Perumangatt, F. Steinlechner, T. Jennewein, and A. Ling, "Entangled photon-pair sources based on three-wave mixing in bulk crystals," *Review of Scientific Instruments*, vol. 92, no. 4, p. 041101, 2021.

[20] C. Perumangatt, T. Vergoossen, A. Lohrmann, S. Sivasankaran, A. Reezwana, A. Anwar, S. Sachidananda, T. Islam, and A. Ling, "Realizing quantum nodes in space for cost-effective, global quantum communication: in-orbit results and next steps," in *Quantum Computing, Communication, and Simulation*, vol. 11699, p. 1169904, International Society for Optics and Photonics, 2021.

[21] S.-K. Liao, W.-Q. Cai, W.-Y. Liu, L. Zhang, Y. Li, J.-G. Ren, J. Yin, Q. Shen, Y. Cao, Z.-P. Li, *et al.*, "Satellite-to-ground quantum key distribution," *Nature*, vol. 549, no. 7670, pp. 43–47, 2017.

[22] M. Polnik, L. Mazzarella, M. Di Carlo, D. K. Oi, A. Riccardi, and A. Arulselvan, "Scheduling of space to ground quantum key distribution," *EPJ Quantum Technology*, vol. 7, no. 1, p. 3, 2020.

[23] L. Mazzarella, C. Lowe, D. Lowndes, S. K. Joshi, S. Greenland, D. McNeil, C. Mercury, M. Macdonald, J. Rarity, and D. K. L. Oi, "Quarc: Quantum research cubesat—a constellation for quantum communication," *Cryptography*, vol. 4, no. 1, p. 7, 2020.

[24] J. S. Sidhu, T. Brougham, D. McArthur, R. G. Pousa, and D. K. L. Oi, "Satellite quantum modelling & analysis software version 1.1: Documentation," *arXiv*, January 2022.

[25] J. S. Sidhu, T. Brougham, D. McArthur, R. G. Pousa, and D. K. L. Oi, "Finite key effects in satellite quantum key distribution," *npj Quant. Inf.*, vol. 8, no. 1, p. 18, 2022.

[26] J. S. Sidhu, T. Brougham, D. McArthur, R. G. Pousa, and D. K. L. Oi, "Key generation analysis for satellite quantum key distribution," in *Quantum Technology: Driving Commercialisation of an Enabling Science II* (M. J. Padgett, K. Bongs, A. Fedrizzi, and A. Politi,

eds.), vol. 11881, pp. 1 – 8, International Society for Optics and Photonics, SPIE, 2021.

[27] J. Yin, Y.-H. Li, S.-K. Liao, M. Yang, Y. Cao, L. Zhang, J.-G. Ren, W.-Q. Cai, W.-Y. Liu, S.-L. Li, *et al.*, "Entanglement-based secure quantum cryptography over 1,120 kilometres," *Nature*, vol. 582, no. 7813, pp. 501–505, 2020.

[28] C.-H. Fung, M. X., and C. H. F., "Practical issues in quantum-key-distribution postprocessing," *Phys. Rev. A*, vol. 81, p. 012318, January 2017.

[29] "Quantum EncrYption and Science Satellite (QEYSSat)." http://qeyssat.ca/, 2022.

[30] A. Scott, T. Jennewein, J. Cain, I. D'Souza, B. Higgins, D. Hudson, H. Podmore, and W. Soh, "The QEYSSat mission: On-orbit demonstration of secure optical communications network technologies," *Proc. SPIE*, vol. 11532, p. 115320H, 2020.

[31] P. Chaiwongkhot, S. Hosseini, A. Ahmadi, B. L. Higgins, D. Dalacu, P. Poole, R. L. Williams, M. E. Reimer, and T. Jennewein, "Enhancing secure key rates of satellite QKD using a quantum dot single-photon source," *arXiv*, 2020.

[32] T. Jennewein, J.-P. Bourgoin, B. Higgins, C. Holloway, E. Meyer-Scott, C. Erven, B. Heim, Z. Yan, H. Hübel, G. Weihs, E. Choi, I. D'Souza, D. Hudson, and R. Laflamme, "QEYSSAT: a mission proposal for a quantum receiver in space," *Proc. SPIE*, vol. 8997, p. 89970A, 2014.

[33] J.-P. Bourgoin, B. L. Higgins, N. Gigov, C. Holloway, C. J. Pugh, S. Kaiser, M. Cranmer, and T. Jennewein, "Free-space quantum key distribution to a moving receiver," *Optics Express*, vol. 23, p. 33437, 2015.

[34] C. J. Pugh, S. Kaiser, J.-P. Bourgoin, J. Jin, N. Sultana, S. Agne, E. Anisimova, V. Makarov, E. Choi, B. L. Higgins, and T. Jennewein, "Airborne demonstration of a quantum key distribution receiver payload," *Quantum Sci. Technol.*, vol. 2, p. 024009, 2017.

[35] E. Anisimova, B. L. Higgins, J.-P. Bourgoin, M. Cranmer, E. Choi, D. Hudson, L. P. Piche, A. Scott, V. Makarov, and T. Jennewein, "Mitigating radiation damage of single photon detectors for space applications," *EPJ Quantum Technol.*, vol. 4, p. 10, 2017.

[36] I. DSouza, J.-P. Bourgoin, B. L. Higgins, J. G. Lim, R. Tannous, S. Agne, B. Moffat, V. Makarov, and T. Jennewein, "Repeated radiation damage and thermal annealing of avalanche photodiodes," *EPJ Quantum Technol.*, vol. 8, p. 13, 2021.

[37] J.-P. Bourgoin, E. Meyer-Scott, B. L. Higgins, B. Helou, C. Erven, H. Hübel, B. Kumar, D. Hudson, I. D'Souza, R. Girard, R. Laflamme, and T. Jennewein, "A comprehensive design and performance analysis of low earth orbit satellite quantum communication," *New J. Phys.*, vol. 15, p. 023006, 2013.

[38] C. Erven, B. Heim, E. Meyer-Scott, J.-P. Bourgoin, R. Laflamme, G. Weihs, and T. Jennewein, "Studying free-space transmission statistics and improving free-space quantum key distribution in the turbulent atmosphere," *New. J. Phys.*, vol. 14, p. 123018, 2012.

[39] T. Vergoossen, S. Loarte, R. Bedington, H. Kuiper, and A. Ling, "Modelling of satellite constellations for trusted node qkd networks," *Acta Astronautica*, vol. 173, pp. 164–171, 2020.

[40] V. M. Acosta, D. Dequal, M. Schiavon, A. Montmerle-Bonnefois, C. B. Lim, J.-M. Conan, and E. Diamanti, "Analysis of satellite-to-ground quantum key distribution with adaptive optics," *arXiv preprint arXiv:2111.06747*, 2021.

[41] L. Roberts, G. Block, S. Fregoso, H. Herzog, S. Meeker, J. Roberts, J. Tesch, T. Truong, J. Rodriguez, and A. Bechter, "First results from the adaptive optics system for lcrd's optical ground station one," in *The Advanced Maui Optical and Space Surveillance Technologies Conference*, p. 3, 2018.

[42] M. W. Wright, J. F. Morris, J. M. Kovalik, K. S. Andrews, M. J. Abrahamson, and A. Biswas, "Adaptive optics correction into single mode fiber for a low earth orbiting space to ground optical communication link using the opals downlink," *Optics Express*, vol. 23, no. 26, pp. 33705–33712, 2015.

[43] C. Scharlemann, M. Tajmar, I. Vasiljevich, N. Buldrini, D. Krejci, and B. Seifert, "Propulsion for nanosatellites," in *32nd International Electric Propulsion Conference, Wiesbaden, Germany, September 2011, IEPC-2011*, vol. 171, 2011.

[44] S. Shafeeq, "Nanosatellite with singapore start-up's thruster deployed into space on spacex mission," *The Straits Times*.

[45] N. Schwartz, D. Pearson, S. Todd, A. Vick, D. Lunney, and D. MacLeod, "A segmented deployable primary mirror for Earth observation from a cubesat platform," in *30th annual AAIA/USU conference on small satellites (SSC16-WK-3)*, 2016.

[46] V. V. Corbacho, H. Kuiper, and E. Gill, "Review on thermal and mechanical challenges in the development of deployable space optics," *Journal of Astronomical Telescopes, Instruments, and Systems*, vol. 6, no. 1, pp. 1 – 30, 2020.

[47] C. J. Pugh, J.-F. Lavigne, J.-P. Bourgoin, B. L. Higgins, and T. Jennewein, "Adaptive optics benefit for quantum key distribution uplink from ground to a satellite," *Advanced Optical Technologies*, vol. 9, no. 5, pp. 263–273, 2020.

[48] D. Dequal, G. Vallone, D. Bacco, S. Gaiarin, V. Luceri, G. Bianco, and P. Villoresi, "Experimental single-photon exchange along a space link of 7000 km," *Phys. Rev. A*, vol. 93, p. 010301, Jan 2016.

[49] B. Dirks, I. Ferrario, A. Le Pera, D. V. Finocchiaro, M. Desmons, D. de Lange, H. de Man, A. J. Meskers, J. Morits, N. M. Neumann, *et al.*, "Geoqkd: quantum key distribution from a geostationary satellite," in *International Conference on Space Optics—ICSO 2020*, vol. 11852, p. 118520J, International Society for Optics and Photonics, 2021.

[50] N. Lütkenhaus, "Estimates for practical quantum cryptography," *Phys. Rev. A*, vol. 59, pp. 3301–3319, May 1999.